Application of Multi-hop Time synchronization on a Network of AUVs Performing Lawn Mower Trajectory

Ansa Shermin S
Dept. of EEE
BITS Pilani K K Birla Goa Campus
Goa, India
p20180017@goa.bits-pilani.ac.in

Sarang C. Dhongdi
Dept. of EEE
BITS Pilani K K Birla Goa Campus
Goa, India
sarang@goa.bits-pilani.ac.in

***Abstract*—This paper presents a use case of multi-hop time synchronization for autonomous underwater vehicles (AUVs) performing lawn mower trajectory. The work showcases a time synchronization protocol that could address mobility in multi-hop underwater scenarios. An existing time synchronization protocol named Doppler-Enhanced time synchronization (DE-sync) protocol is chosen and extended to an application-specific multi-hop scenario. It further considers the error analysis in the elapsed time duration after message exchanges in each hop. Simulations have been performed using MATLAB. It is observed that DE-sync shows better performance in terms of synchronization error than the other similar protocols. It is also found that error increases with the number of hops but with limited bounds.**

***Index Terms*—multi-hop, time synchronization, autonomous underwater vehicles, lawn mower**

I. Introduction

For most cooperative underwater missions, there is a great need for the nodes in the network to share a common notion of time. These nodes must be time synchronized to achieve the shared goals of a cooperative mission. However, the clock in the sensor nodes is made of crystals prone to intrinsic drift, and additionally, different offsets lead to synchronization errors with time advancements. Therefore, the nodes must be synchronized to the reference node with an ideal reference time. This paper presents the multi-hop time synchronization of underwater mobile sensor networks (UWMSN).

Usually, the underwater networks deployed for greater depths are not necessarily single-hop networks. The formation of multi-AUVs is often used. Therefore, it is necessary to devise multi-hop synchronization techniques for these mobile networks. Many protocols available in the literature are suitable for mobile networks [1], [2]. Nevertheless, most are either complex or only consider the clock offset resulting in a larger synchronization error. Meanwhile, the DE-sync proposed in [3] is a good choice for these networks, as it is a skew-based technique that helps to achieve a better performance than the other similar existing protocol. This work extends the DE-sync protocol applied for a specific multi-hop UWMSN topology is shown in Figure 1. The process starts with the unsynchronized node AUV B getting synchronized to a reference node at the surface, i.e., Buoy A. After a certain interval, the newly synchronized node will act as a reference node to the next hop node. The synchronization process will continue till all the nodes in the network are synchronized.

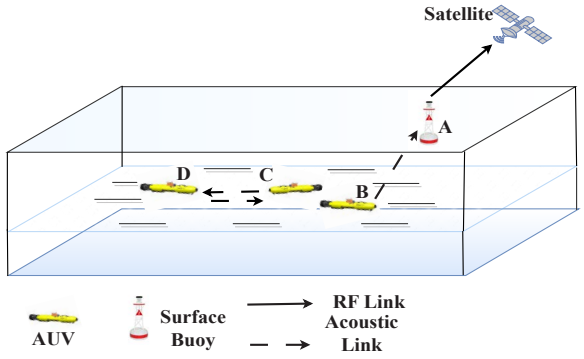

Fig. 1. Multi-hop UWMSN network

This paper analyses how the DE-sync is applied to a specific topology of mobile nodes. Further, the results are validated using MATLAB. The organisation of the paper is described as follows. Section II presents the related works. In Section III multi-AUV network's topology and the DE-sync implementation are described. Section IV gives the error analysis of the implemented protocol, and Section V shows the results and discussion. Finally, Section VI concludes the paper.

II. Related Works

Various time synchronization protocols in the literature for underwater networks support large propagation delays and mobility of network nodes. TSHL is the first method of this kind to address the high latency in underwater networks, though it is meant for static networks [4]. In contrast, MU-sync is a cluster-based protocol that has addressed the mobility of UWMSN [5]. It operates in two phases for the skew and

offset estimation. This protocol claims to reduce the need for frequent resynchronization. However, MU-Sync seems less energy efficient than TSHL due to the large no. of message exchanges.

Another algorithm proposed to assist mobility is Mobi-Sync [2]. Here, for enhancing the accuracy of fast-changing propagation delay the spatial correlation of sensor node motion is considered. The network consists of GPS-equipped surface buoys, high-precision super nodes that can achieve synchronization, and standard nodes that implement time synchronization. A correlation model is used here to calculate the node's velocity to the super node. While estimating the time-varying latency, developing precise correlation models between the nodes is particularly challenging.

D-Sync proposed in [6] adds the physical layer information corresponding to mobility. Doppler shift is estimated here. The primary limitation resulting from motion in underwater communication is the Doppler shift. This demands the estimation and compensation for the Doppler effect. The Doppler shift determines the timing uncertainty due to mobility since it is useful in providing information about the node's velocity. Although it determines the Doppler scaling factor, the clock skew is not considered here. Thus, it decreases time synchronization accuracy and lowers the Doppler shift estimation accuracy.

A time synchronization protocol called DA-Sync [1] offers a framework to more accurately predict the Doppler shift brought on by mobility by considering clock skew. The Kalman filter is used for velocity estimation to improve time synchronization. Two linear regression runs are used to calibrate the clock skew and offset. However, the assumptions regarding the sound speed as a function of various factors like temperature, salinity, and depth, when directly applied to the synchronization, cause extra errors in this protocol.

While the DE-Sync method described in [3] accounts for clock skew for the Doppler scale factor estimation and further uses linear regression as a replacement to get the estimate of clock skew and offset. Therefore, in this paper, DE-sync is taken as a choice for implementation. In this work, DE-sync and D-sync are considered for performance comparisons, as D-sync is much similar to DE-sync. Even though the D-sync considers the Doppler shift, it has not considered the clock skew for estimating the Doppler effect. Instead of the Doppler scale factor, it uses relative velocity. The performance of both protocols is present in Section V.

III. Topology Description for Multi-AUV network

The need for multi-AUV networks usually arises for wide-area surveillance, such as plume monitoring applications. For instance, consider the occurrence of the Deepwater Horizon blowout [7] at the MC252 Macondo well site in the Gulf of Mexico. The plume spreads 35 km in length, has a Depth of 1100 m, and lasts for months. These sorts of applications require multiple AUVs for faster mission completion. Therefore, this work presents the time synchronization of AUVs in such a scenario.

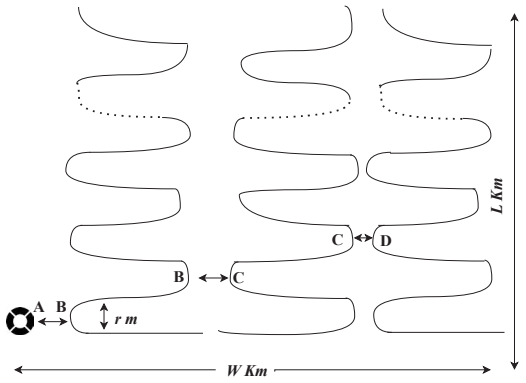

Fig. 2. AUVs traversing in lawn mower trajectory

The topology built here is for a two-dimensional deployment, where the area $W \times L$ has to be sampled by n AUVs (here, say 3). The AUVs are expected to follow the lawnmower trajectory, as shown in Figure 2.

The area is divided into three subsections with L/d levels; d is the swath width. Each AUV will start from its initial position and must traverse the W/n distance horizontally and L/d vertically to reach the next level. Thus, there are L levels for each AUV. The distance between each subsection is maintained to avoid any potential collisions. The AUVs can communicate when they come in contact with each other, usually during vertical traversal. Here, an area of $(15Km \times 10Km)$ is considered with each subsection of about $(4Km \times 10Km)$. Since it is difficult for upright vertical traversal for AUV, it can take a semicircular path with a curvature radius of r m.

It is assumed that one buoy is available at the water surface, connected with the GPS (hence, having a perfect clock). Moreover, it is considered that the buoy is deployed only at the reach of the first AUV, making room for the buoys to only communicate with the 1^{st} AUV. (The AUVs are deployed 200 m below the water surface). Figure 2 shows a surface buoy denoted by A and three AUVs, B, C, and D, respectively. At first, AUV B will get synchronized to buoy A. After the first-hop, node B acts as a reference node for node C, and the process continues. After the mission completion, the AUVs are taken back to the surface station. The message exchanges for multi-hop synchronization are described in Figure 3.

The time of any unsynchronized node B is given by;

$$T = \alpha t + \beta \tag{1}$$

In Equation (1), T is the time for the unsynchronized node. The relative skew and offset are denoted by α and β . Variable t corresponds to the ideal time of the reference node. The relative motion of the mobile entities is obtained in the DE-sync by estimating the Doppler scale factor. There are three phases for the DE-sync, namely i) the data collection phase, ii) the linear regression phase and iii) the calibration phase. The Doppler factor is estimated from the physical layer information obtained from the message exchanges between the nodes in the data collection phase. While the message is exchanged with the

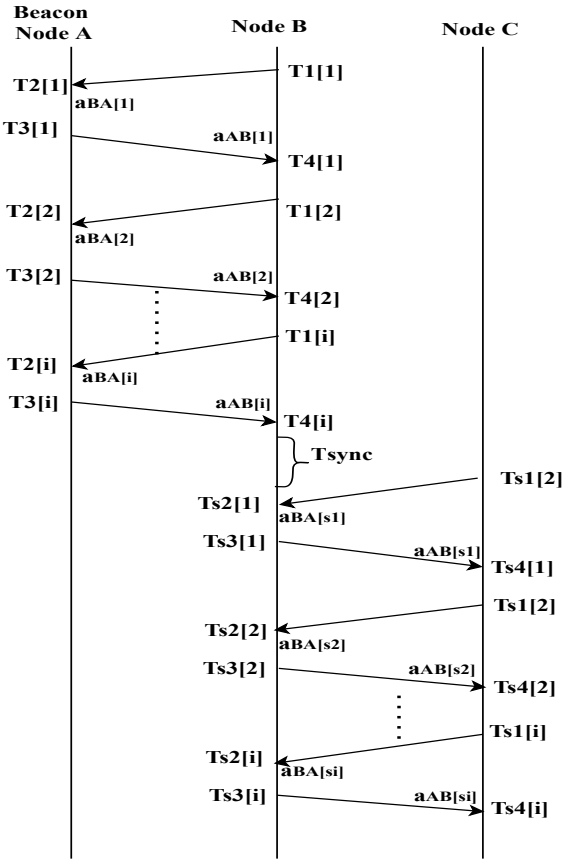

Fig. 3. Message exchanges in multi-hop synchronization

reference node, the unsynchronized node will collect the time stamps from the messages along with the Doppler scale factor. The clock and offset of the unsynchronized nodes are obtained during the first regression. During the calibration process, the unsynchronized node performs calibration by replacing the initial skew and offsets with the obtained values to obtain the final values of skew and offset.

A. Considering the effect of mobility in clock skew

Consider a scenario where the reference node A, (this is a buoy with an ideal clock) sent a message to the unsynchronized node (AUV) B, which has an intrinsic time drift, leading to a skew in node B. The baseband signal sent from node A to node B x_{AB} is given by Equation (2). The signal received, y_{AB}, is the sum of the signal obtained from multiple paths.

$$y_{AB}(n) = \sum_{p=1}^{Np} A_p x_{AB}((1 + a_{AB})n - \tau_p) \tag{2}$$

N_p corresponds to the path number of the multipath signal, a_{AB} the Doppler scale factor, and A_p and τ_p are the amplitude and delay of the p^{th} path, respectively. The Node B's clock will drift as per Equation (1), i.e., if the time of A is expressed as samples of $t[n] = nT_s$, then for node B, the time is expressed as $t[n] = \alpha n T_s$. The measured Doppler scale factor a_{AB} is the combined effect of the clock skew and relative motion between the nodes so that it can be expressed as $1 + a_{AB} = \alpha\,(1 + a_m)$. Where a_m is the Doppler scale factor due to mobility. Similarly, for node A, after the message reception from B, node A's time is expressed as $t[n] = (nT_s)/\alpha$. So, the measured Doppler scale factor by node A a_{BA}, will be $1 + a_{BA} = \frac{(1+a_m)}{\alpha}$.

So, a_m gives the Doppler scale factor due to mobility, and it can be expressed as,

$$a_m = \begin{cases} ((1 + a_{AB})/\alpha) - 1 & A \to B \\ \alpha\,(1 + a_{BA}) - 1 & B \to A \end{cases} \tag{3}$$

B. Implementation of DE-sync on the mentioned topology

While implementing the DE-sync in the mentioned topology, the message exchange is initiated by node B. Node B sends a synchronization request message to node A at time T_1 after marking its timestamp from the MAC layer. Node A receives the message at time T_2 and marks the receiving time stamp and the Doppler shift factor from node B, a_{BA}. Then node A will back-off for a certain time called $T_{backoff}$ and send a response message at T_3 containing the timestamps T_2, T_3 and the Doppler shift factor a_{BA}. At the time T_4, node B receives a synchronization message having T_1, T_2, T_3 , a_{BA}, and further measures Doppler shift factors from node A, a_{AB}. The process is described in Figure 3. A certain set of equations are derived in DE-sync to find the skew and offset of the nodes. From Equation (1), the timing equations are as follows,

The reference time t_1, t_2, t_3, t_4 are defined as follows,

$$T_1 = \alpha t_1 + \beta, T_4 = \alpha t_4 + \beta$$
$$T_2 = t_2, T_3 = t_3$$
$$t_2 = t_1 + \tau_1, t_4 = t_3 + \tau_2$$
$$T_1 = \alpha\,(T_2 - \tau_1) + \beta$$
$$T_4 = \alpha\,(T_3 + \tau_2) + \beta$$

Where τ_1 and τ_2 are the propagation delays from B to A and A to B, respectively. Considering the realistic assumptions about mobility, the round trip propagation delay is not necessarily equal to halfway round trip time, i.e., $\tau_1 \neq \tau_2$. The values for τ_1 and τ_2 are solved from the above set of time constraints. Substituting these values in the node's local timings, i.e., T_1 and T_4, will give the basic Equation for linear regression, Equation (4). (For detailed derivation, interested readers can refer [3])

$$\begin{aligned} 2T_1 + T_4\,(2 - (a_{AB} + a_{BA})) = \alpha\,(T_2\,(2 - (a_{AB} + a_{BA})) \\ +2T_3 + \beta\,(4 - (a_{AB} + a_{BA})) + \varepsilon \end{aligned} \tag{4}$$

The Doppler scale factor, at time t_2 measured by node A is $a_{BA} = v_{BA}/c$. While at t_4, node B measured it as $a_{AB} = v_{AB}/c$. v_{AB} and v_{BA} are the relative velocities measured from A to B and B to A respectively. And c denotes the sound propagation speed. The average of the relative velocity of the nodes v_m, (termed as interpolation) is considered here. It is expressed as $v_m = 0.5 \times (v_{AB} + v_{BA}) + \epsilon_v$, i.e., $v_m = 0.5 \times c \times$

$(a_{AB} + a_{BA}) + \epsilon_v$, where ϵ_v denotes an error due to random noise and the interpolation error.

The linear regression is then performed based on Equation (4) to estimate the skew and offset while considering the mobility of the nodes, which gives,

$$\begin{aligned} \hat{\Lambda} = [\hat{\alpha}, \hat{\beta}]^T &= \left(H^T H\right)^{-1} H^T Y \\ Y[i] &= 2{T_1}^i + {T_4}^i \left(2 - \left({a_{AB}}^i + {a_{BA}}^i\right)\right) \\ H[i,1] &= 2{T_3}^i + {T_2}^i \left(2 - \left({a_{AB}}^i + {a_{BA}}^i\right)\right) \\ H[i,2] &= \left(4 - \left({a_{AB}}^i + {a_{BA}}^i\right)\right) \end{aligned} \tag{5}$$

Where $[\hat{\alpha}, \hat{\beta}]^T$ gives the estimates of the clock skew and offset after performing N rounds of message exchanges from Equation (5). Here, Y corresponds to a $(N \times 1)$ matrix and H is a $(N \times 2)$ matrix, and their entries will be obtained from Equation (5). For the initial round, the skew is taken as 1 and offset as 0. After getting the estimated values from the first round of the message exchange, the skew and offset are calculated. Calibration will be performed using these values until the set threshold is achieved.

IV. Error Analysis

The error in the DE-sync mainly constitutes the random noise and the interpolation error [6]. The interpolation error is due to the fact that the Doppler measurements are not continuously available. Instead, it is taken as the average of the two measured Doppler scale factors obtained at the end of each message transmission. From Equation (4), the error ε is expressed as

$$\begin{aligned} \epsilon &= \frac{\epsilon_v}{c} \times \alpha \times (T_4 - \alpha T_2 - \beta) \\ \varepsilon &= \frac{\varepsilon_v}{c} \times \alpha \times (T_3 - T_2 + \tau_2) \\ \epsilon &= (\epsilon_{\text{noise}} + \epsilon_{\text{interp}}) \times \alpha \times (T_{\text{backoff}} + \tau_2) / \text{c} \end{aligned} \tag{6}$$

Where $\frac{\epsilon_v}{c}$ is introduced during the conversion of the Doppler scale factor, which mainly constitutes random noise and interpolation error [6]. The duration $(T_3 - T_2)$ is termed as the response time $(T_{backoff})$.

A. Error in Multi-Hop time synchronization

In a multi-hop network, the error accumulates while advancing from one hop to another. Knowing the accumulated error to some bounds is necessary to keep the required precision of the given application. Consider Figure 3, which represents the message exchange of two hops in a network. The error analysis for the first hop is done as shown above. An interval named t_{sync} is defined between the two hops in the figure. For a better error analysis, it is also important to determine the clock drift in that elapsed time duration. Therefore, while determining the second hop error, the total error has translated to,

$$E_{tot} = E_{rrFH} + E_{rrtsync} + E_{rrSH} \tag{7}$$

Where, E_{rrFH} is Error in the first hop, $E_{rrtsync}$ the Accumulated error in the t_{sync} duration and E_{rrSH} Error in the second hop.

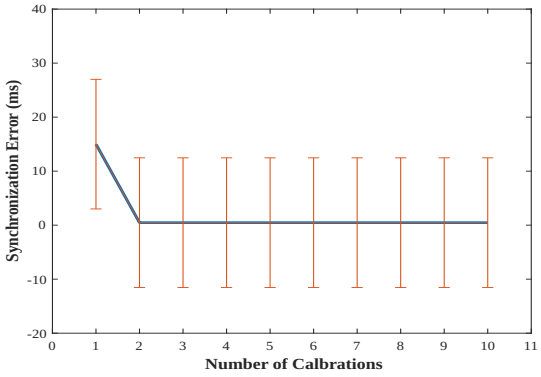

Fig. 4. Performance with no.of calibrations

B. Finding the Clock Drift in t_{sync}

Consider the underwater scenario where the mobile vehicles/nodes are equipped with any commercially available oscillator, as shown in Table 1. From this table, the drift that occurred during the t_{sync} can be easily determined. For instance, assuming that the vehicles are using the TXCO oscillator manufactured by Sea Scan, it will create a drift of 1 ms in 14 hours. Using the oscillator OXCO of Trimble Navigation, Ltd. could produce only an error of 2.8 ns/s, but with a higher power trade-off [8]. Depending upon the required precision and nature of the application, one has to choose the resynchronization period [9]. The resynchronization interval determines the maximum tolerance for synchronization error. Suppose the sending and receiving vehicles use the crystal with a maximum frequency error of ±ef ppm. Then the error in the resynchronization interval ϵ is given by Equation (8)

$$\epsilon = \Delta t \left(\frac{1}{1 - e_f} - \frac{1}{1 + e_f} \right). \tag{8}$$

Where Δt is the resynchronization interval. The above equation can be further approximated to,

$$\epsilon \approx \Delta t \times 2e_f \tag{9}$$

It is to be noted that the t_{sync} should be less than Δt in order to avoid frequent resynchronization. Depending upon the stability of the crystals used in the oscillators the resynchronization interval can range from several hours to days.

V. Results and Discussion

DE-sync is analysed for the mentioned topology in the Region of Interest (RoI) $15Km \times 10Km$. Simulations are done using MATLAB. The comparisons of DE-sync and D-sync for various parameters are made in this section. The simulation parameters used are shown in Table II.

- Number of calibration- Figure 4 shows the synchronization error with no. of calibrations. As discussed, for the first run of linear regression, the ideal conditions for clock skew and offset are assumed; therefore, the Doppler scale factor is not corrected. This results in a larger synchronization error in the first run. From the next run

TABLE I
COMMERCIALLY AVAILABLE OSCILLATORS SUITABLE FOR AUV APPLICATIONS [8]

Manufacturer	Model	Type	Drift	Power	Size
SeaScan,	Inc. SISMTver 4.0	TXCO	20 ns/s	5 mW	71 × 45 × 23 mm
A.C.S.A.	GIB-USC-2-A	TXCO	20 ns/s	600 mW	148 × 94 × 34 mm
Trimble Navigation, Ltd.	Mini-T	OXCO	2.8 ns/s	1.75 W	128 × 27 × 19 mm

TABLE II
PARAMETERS FOR SIMULATION

Parameters	**Value**
Max. distance between AUVs d_{max}	1 Km
Max. relative velocity v_{max}	5 m/s
Max. relative acceleration a_{max}	$0.1m/s^2$
Response Time $t_{backoff}$	2 s
No. of messages exchanges for linear regression	20

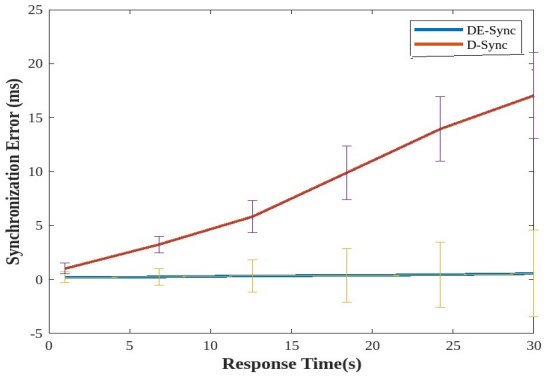

Fig. 5. Performance with response time

onwards, calibrations are done using the estimated values, which reduces the error.

- Response Time- Figure 5 shows the performance of sync-error with response time. The mean and standard deviation for D-sync and DE-sync is plotted by varying the response time from 1 s to 25 s. The error usually increases with the response time as the Doppler measurements

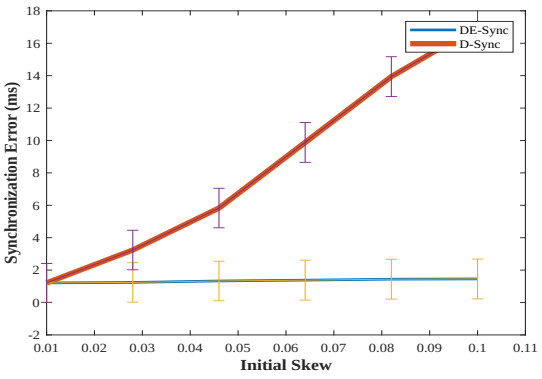

Fig. 6. Performance with initial skew

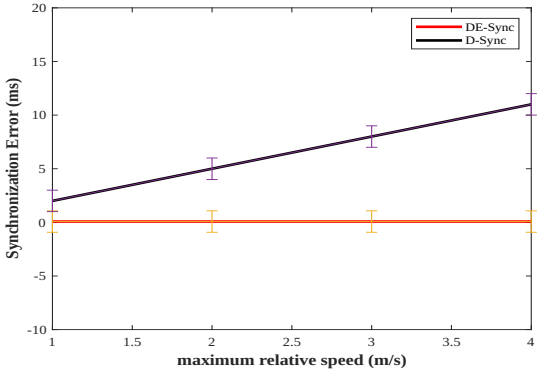

Fig. 7. Performance with relative speed

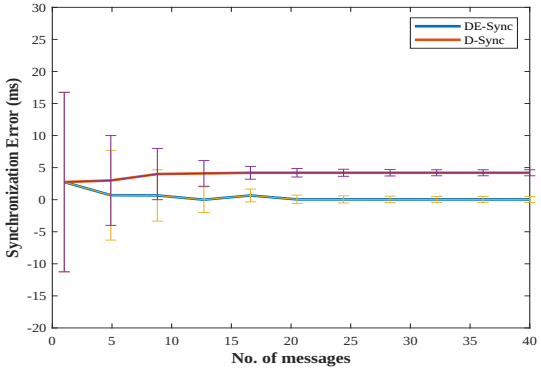

Fig. 8. performance vs number of messages

are available only when the messages are exchanged. Unlike D-sync, the error in the DE-sync is consistent as it considers the skew in estimating the Doppler scale factor.

- Initial Skew- Figure 6 shows the performance of the initial skew; the inherent skew ranges from 50 to 10^6 ppm. However, this work only considers a relatively larger skew from 0.02×10^6 ppm. It is observed that DE-Sync shows a more consistent performance than D-sync with a larger skew.
- Effect of Mobility- The nodes' speed varies between 1 m/s to 5 m/s. The error induced in D-sync is with respect to Equation (10). The performance with relative speed is shown in Figure 7. For the unsynchronized node, the α will not be 1, so the error will increase with v_m. However, as it considers the skew in estimation, DE-sync shows

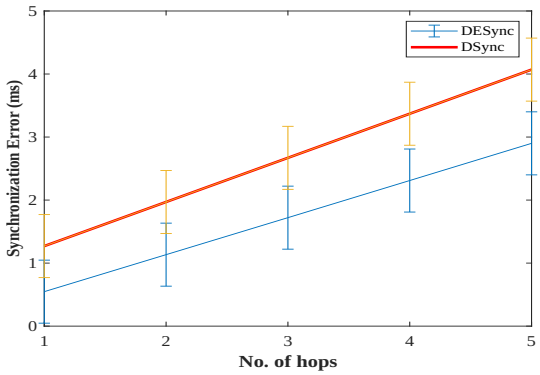

Fig. 9. Error in multi-hop

consistent performance.

$$\varepsilon_a = 0.5 \times \left(\alpha + \frac{1}{\alpha} - 2\right) \times (v_m + c) \qquad (10)$$

- No. of message exchanges- Figure 8 shows the mean and standard deviation with the no. of message exchanges varying from 5 to 45. With the increase in no. of messages, the standard deviation decreases in both cases. However, the relative velocity of the vehicles increases with an increase in message exchange in D-sync, which further increases the mean of error. The DE-sync possesses a lower mean than the D-sync.
- Error in multi-hop- Figure 9 shows the effect of error in multi-hop topology, as shown in Figure 2. It is shown that the error increases with the multiple hops in D-sync and DE-sync. The first hop error is determined based on both cases' corresponding error analysis schemes. Considering the second hop, the error is accumulated, as shown by Equation (6). The error in the D-sync is greater than DE-sync from their corresponding error equations. This work has emphasised the same methodology for determining the multi-hop error in both cases. Considering Figure 2, the synchronization starts when the first AUV B sends a synchronization message to Buoy A (reference node). The mean error in DE-sync for the first hop was 0.547 ms, and 1.3 ms for D-sync. For the second hop, AUV B is the reference node, and it has to travel a distance of 4 Km before synchronising node C. Suppose the AUV B is travelling at 2 m/s; the time taken for traversing 4 Km is 4 Km/2 = 2000 s. It is considering t_{sync} as 2000 s and assuming that the AUV is using the crystal with the drift of 20 ns/s. Therefore the drift in this duration was $2000 \times 20ns$. The error in the second hop is, therefore, 1.13 ms for the DE-sync and 1.883 ms for the D-sync. So, for n-hops, Equation (6) transforms into

$$E_{Network} = d \times E_{ch} + (d-1) \times E_{rrtsync} \qquad (11)$$

$E_{Network}$ is the total error the network can tolerate, d is the no. of hops and E_{ch} is the error in the corresponding hops, $E_{rrtsync}$ is the error during t_{sync}. The error increases with no. of hops for both the DE-sync and D-sync.

VI. Conclusion

This work mainly addressed the multi-hop time synchronization of mobile underwater nodes. An existing protocol named DE-sync is modified here for a multi-hop AUV network traversing a lawn mower trajectory. As DE-sync considers the clock skew for estimating the Doppler scale factor, which accounts for the mobility of nodes, it shows consistent results when compared with a similar protocol named D-sync. Further, this work performs multi-hop error analyses in the mentioned topology. Besides finding the error in linear regression, knowing the clock drift after an elapsed time duration is important for more precise error analysis. This paper considers the drift after synchronization while progressing towards the multi-hop network. It is observed that the error increases with the no. of hops with limited bounds.

ACKNOWLEDGMENT

Sarang Dhongdi acknowledges the funding support received for his Strategic Research Project from BITS BioCyTiH Foundation, a Section 8 company of BITS Pilani under the National Mission of Interdisciplinary Cyber-Physical Systems (NM-ICPS), Department of Science and Technology (DST), Government of India.

References

[1] J. Liu, Z. Wang, M. Zuba, Z. Peng, J.-H. Cui, and S. Zhou, "DA-Sync: A Doppler-Assisted Time-Synchronization Scheme for Mobile Underwater Sensor Networks," *IEEE Transactions on Mobile Computing*, vol. 13, no. 3, pp. 582–595, 2013.

[2] J. Liu, Z. Zhou, Z. Peng, J.-H. Cui, M. Zuba, and L. Fiondella, "Mobi-Sync: Efficient Time Synchronization for Mobile Underwater Sensor Networks," *IEEE Transactions on Parallel and Distributed Systems*, vol. 24, no. 2, pp. 406–416, 2012.

[3] F. Zhou, Q. Wang, D. Nie, and G. Qiao, "DE-sync: A Doppler-Enhanced Time Synchronization for Mobile Underwater Sensor Networks," *Sensors*, vol. 18, no. 6, p. 1710, 2018.

[4] A. A. Syed, J. S. Heidemann, *et al.*, "Time Synchronization for High Latency Acoustic Networks," in *Infocom*, vol. 6, 2006, pp. 1–12.

[5] N. Chirdchoo, W.-S. Soh, and K. C. Chua, "MU-Sync: A Time Synchronization Protocol for Underwater Mobile Networks," in *Proceedings of the third ACM international workshop on Underwater Networks*, 2008, pp. 35–42.

[6] F. Lu, D. Mirza, and C. Schurgers, "D-sync: Doppler-based Time Synchronization for Mobile Underwater Sensor Networks," in *Proceedings of the Fifth ACM International Workshop on UnderWater Networks*, 2010, pp. 1–8.

[7] R. Camilli, C. M. Reddy, D. R. Yoerger, B. A. Van Mooy, M. V. Jakuba, J. C. Kinsey, C. P. McIntyre, S. P. Sylva, and J. V. Maloney, "Tracking Hydrocarbon Plume Transport and Biodegradation at Deepwater Horizon," *Science*, vol. 330, no. 6001, pp. 201–204, 2010.

[8] R. M. Eustice, H. Singh, and L. L. Whitcomb, "Synchronous-clock, one-way-travel-time acoustic navigation for underwater vehicles," *journal of field robotics*, vol. 28, no. 1, pp. 121–136, 2011.

[9] A. Elsts, S. Duquennoy, X. Fafoutis, G. Oikonomou, R. Piechocki, and I. Craddock, "Microsecond-accuracy time synchronization using the ieee 802.15. 4 tsch protocol," in *2016 IEEE 41st conference on local computer networks workshops (LCN Workshops)*. IEEE, 2016, pp. 156–164.